Mathematical modelling of geogrid reinforced embankments subject to high energy rock impacts

A. Carotti
Politecnico di Milano, Milano, Italy

D. Peila, C. Castiglia
Politecnico di Torino, Torino, Italy

P. Rimoldi
Tenax S.p.A., Viganò Brianza (LC), Italy

Keywords: Walls, Numerical modeling, Geogrid, Landslides, Performance evaluation.

ABSTRACT: Geogrid reinforced embankments find more and more applications as barriers against rock fall, for the protection of all kind of infrastructures.The dynamic behavior of these structure benefits of three specific energy absorption mechanism:
- an increase of the elastic stiffness of the embankment, due to the high tensile modulus of geogrids;
- an increase of the viscous damping of the embankment, due to the elasto-plastic properties of geogrids;
- an increase of the viscous damping of the embankment, due to the Coulombian friction dissipation that is made possible by the soil-geogrid interaction.

The dynamic behavior of geogrid reinforced embankments subject to impulsive loads has never been modeled before.The proposed mathematical model is based on sound mechanical principles and is validated with the results of full scale high energy impact tests.The model allows a better understanding of the dynamic behavior of geogrid reinforced embankments subject to the impacts of heavy rocks with high speed, and it constitute a first engineering tool for the design of such structures.

1 INTRODUCTION

When dealing with the problem of protecting civil infrastructures, such as highways or inhabited areas, the large amount of protections to be installed makes the problem of their cost more and more important; moreover, the length of the installation often forces the designers to choose rock fall protection devices which feature high energy absorption to deal both with high energy impacts and with “swarms” of falling boulders, and which require strong maintenance or reparations.

This is why, whenever the morphology of the area makes it possible, reinforced earth walls are sometimes preferred to net fences. According to Yoshida and Nomura (1998), the metric cost for high energy absorption fences varies from 2000 to 9000 US$, covering a range of energies going from 500 to 2000 kJ (even if some net fences able to absorb energies up to 3100 kJ have been developed and tested in Europe), while GeoRock Walls (a patented device consisting in a reinforced earth wall with some protecting cushions filled of sand) can cope with a wider energy range (up to 2500 kJ) for approximately half the price (fig.1).

It must be observed that the knowledge of the behaviour of a reinforced ground wall subject to dynamic impacts is still limited, and many researches are under development all around the world.

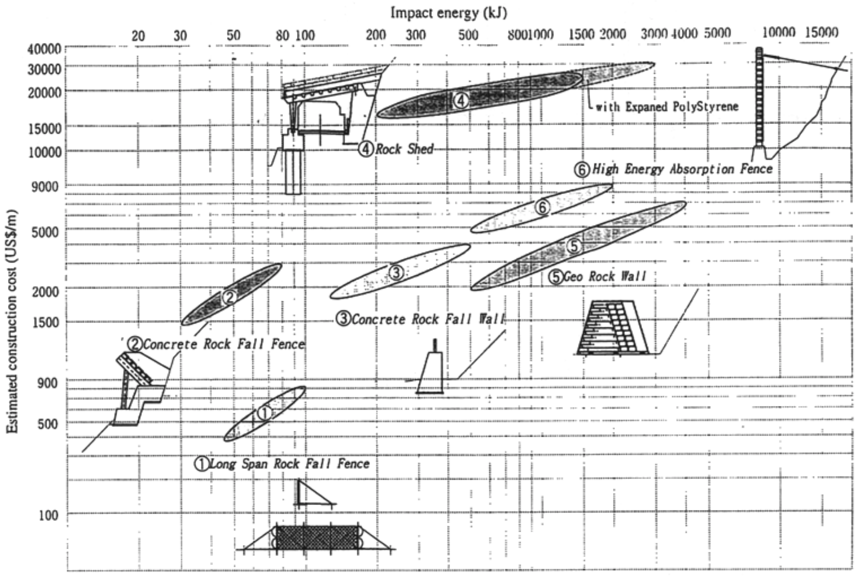

Fig. 1: Energy vs cost plot for common rockfall protection devices (Yoshida et al., 1998)

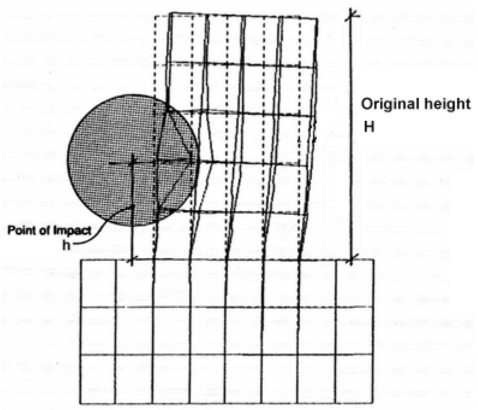

Fig. 2:Screenshot of the numerical model (Burroughs et al.,1993)

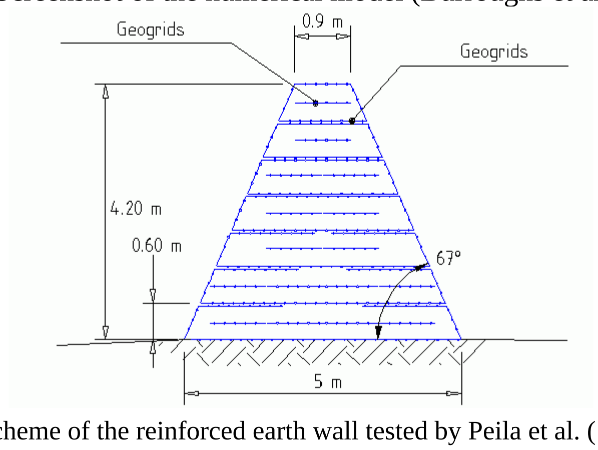

Fig. 3:Scheme of the reinforced earth wall tested by Peila et al. (1999)

1.1 *The role of numerical modeling*

Obviously, the best way to understand the energy dissipation mechanisms and then to predict the dynamic response of a reinforced earth structure is to study it in full scale, testing its performance simulating real impacts with high-speed boulders. Furthermore, numerical modeling of real structures plays an important role in this research phase.

Of course, the feasibility of every mathematical model has to be verified comparing its results with those obtained from real field tests. If the models fit it is possible to analyze more deeply the mathematical one to study the global stress and strain fields and their evolution during the simulation time or to highlight local plasticity.

It is also possible to modify material properties to carry out parametrical analyses, obtaining a wide range of results from a single full-scale test.

1.2 *Numerical modeling of rock fall walls*

Although several models of earth walls have been developed during the last decade just few of them are focused on the evaluation of the dynamic behavior of the structure during rock impacts.

The only scientific work known to the authors is the one which has been carried out by Burroughs, Henson and Jiang (1993) which simulates a 3-dimensional impact of a mass on a wall made out of homogeneous, continuous and elastic-plastic material (fig. 2).

Through a parametric analysis, a design chart for back side deformation after the impact has been drawn, but the hypothesis of continuity of the material did not allow any investigation on reinforcements strains and stresses.

The model discussed in this paper is instead based on the results obtained by Peila et al. (1999) during several full scale tests on reinforced embankments.

1.2.1 *Brief description of the full scale test phase*

The test was carried out in the test site of Meano (TN), a specially built up facility where steel-reinforced concrete blocks can be thrown with a free fall trajectory (fig.4). This technique allows to easily calibrate boulder's impact direction and speed, which proves to be useful when standard test condition have to be applied to different crashes.

Boulders with different sizes are available (featuring weights up to 9000 kg) so that several kinetic energies can be developed with the same impact velocity. In the test which has been used for the back analysis phase a block with a weight of 4998 kg impacted the front face developing an energy of 2511 kJ, but more recently up to 5000 kJ impact tests have been carried out.

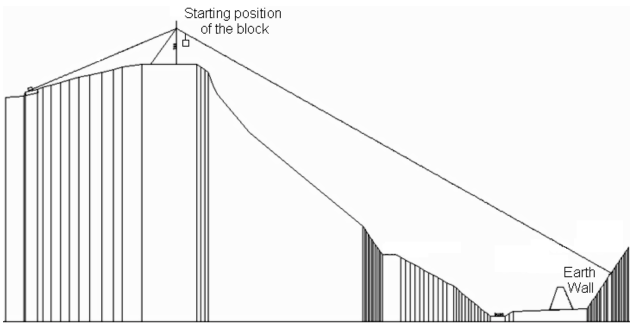

Fig. 4: scheme of the test site.

1.3 *Closed form model*

For the design of reinforced soil rock-fall protection walls and embankments, it is important to afford a closed form model able to provide easily and quickly the order of magnitude of forces and deformations due to a given impact.

The closed form mathematical model must be easily implemented on computer and must be stable and feasible, that is it must provide good results even when facing variations of the main parameters of the model itself.

Such models are only in the early stages of development. To the Author's knowledge no closed form mathematical model of reinforced soil rock fall protection walls and embankments have been published so far. Therefore, in the present paper the Authors present some general principles for providing a guide to researchers in this field.

2 NUMERICAL MODELS

The code used for the simulation is ABAQUS/Explicit ©(Hibbit, Karlsson et al., 1998) which allows the evaluation of finite elements meshes in a 3-dimensional, dynamic, non-linear field using an explicit Euler solving algorithm.

Several different models have been set up. The first one that has been used to model the ground wall tested in the full scale experience (fig. 3), which was 10 meters long, with an height of 4.2 meters and two faces with a 67° tilting. Seven levels of compacted earth composed it with wrapped geogrids used as reinforcements. To simulate the soil, 8-node brick finite elements have been used, while the geosynthetic interfaces are simulated by 4 node membrane elements. The final mesh was made out of 15120 brick and 1820 shell elements (fig. 5).

Drucker-Prager yield criterion has been chosen to describe the plastic behavior of the ground while, on the basis of the observations made in the full-scale test, the geogrids were supposed to be perfectly elastic; all the required parameters (table 1) have been evaluated through laboratory tests (Peila et al., 1999). The impacting boulder has a cubic shape and it is modeled as infinitely stiff.

Table 1: Geotechnical parameters of the soil fill.

c' [KPa]	ϕ' [°]	ϕ' [°]*	γ'[KN/m^3]*
9	33.7	44	2110
(*) after compaction			

After the back analysis of the full scale test, two other numerical models have been developed: the first one simulates the impact of a boulder on a non reinforced ditch, with the aim of evaluating the role of the reinforcements on the dynamic resistance of the structure, while the second one features the same geometry of the full scale test with far worse geotechnical parameters.

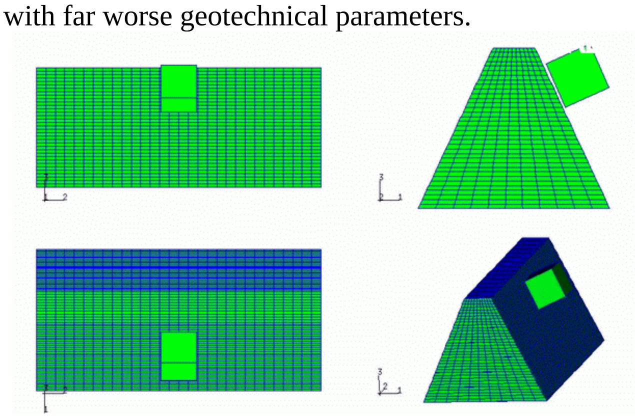

Fig. 5: 3d view of the mesh.

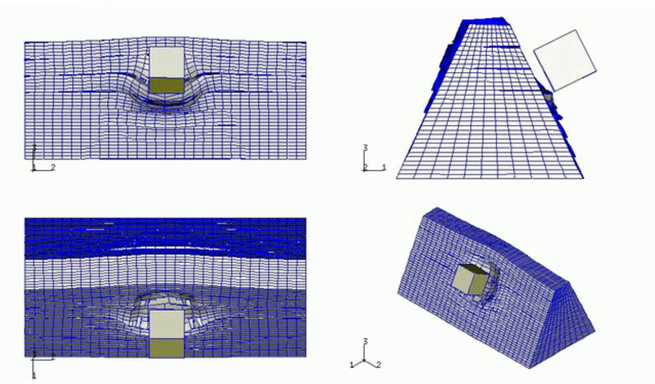

Fig. 6 : deformed mesh of the first model

2.1 *Results of back analysis*

The boulder, with a mass of 5000 kg impacting with a speed of 24 m/s in the vertical direction and of 20 m/s in the horizontal one, has been arrested by the wall.

Table 2: full scale Vs simulated results

	Contact Time [ms]	Front Deformation [cm]	Back Deformation [cm]
Full Scale	~160	~40	~23
FE model	800	35	25

It caused a differential displacement of the soil levels as observed in the full-scale test (fig.6); also, simulated data show a good comparison with the real test . (table 2)

It is interesting to analyze the peak stresses developed in the reinforcements: excluding the impact area, where the large strains bring to very high stresses, a strip of higher tensile stresses can be observed in the center, seemingly related to the impact (fig. 7).

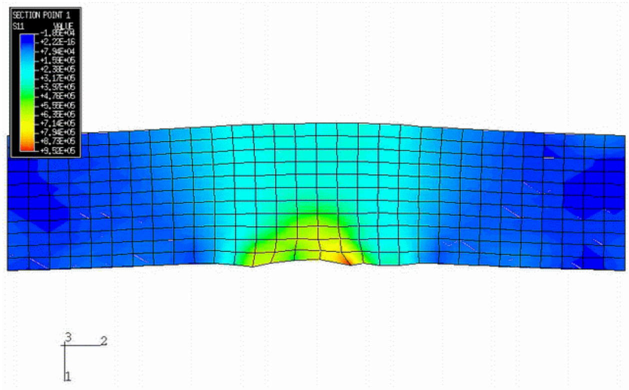

Fig. 7: peak stresses in the 6th geogrid.

Even if those stresses never exceed the tensile limits of the HDPE geogrids used in the actual test (50 kN/m), in several areas the safety factor (allowed stress versus actual stress ratio) of the reinforcements drops very near to 1, thus highlighting a local dynamic effect that cannot be predicted in any way by analytical methods.

2.2 *Model without reinforcements*

In this simulation, a boulder, similar to the one previously described, impacts on a non reinforced earth barrier with a speed of 28 m/s.

Obviously, wall geometry must be compliant with the absence of reinforcements, so the face dip has been lowered down to 45°, resulting in a more “massive” structure with a 10 meters basal thickness which proves to be able to stop the rock with small deformations (fig. 8) of the front face (26 cm) while the back face does not show any relevant displacement.

Having no internal anisotropy due to geogrid strata, the wall does not show the differential displacements previously illustrated (fig.9), and seems to behave in a more predictable manner for which analytical methods for the evaluation of projectile penetration can be feasible (Petry, 1968, Kar, 1978, Mayne et al., 1984).

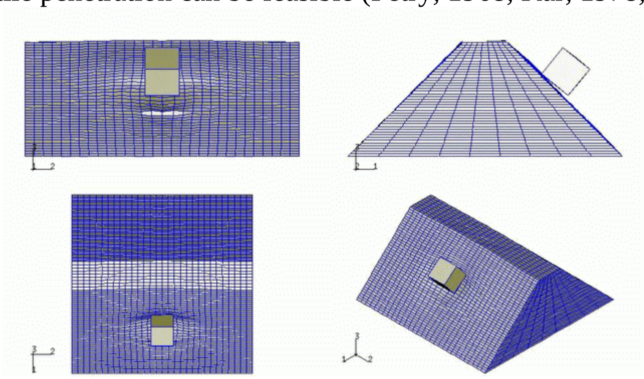

Fig. 8: deformed mesh of the non reinforced earth wall.

2.3 *Model with worse soil parameters*

In this simulation the soil has been supposed to have no cohesion and an internal friction angle 35% lower than the back analysis one, while everything else has been kept identical to the first test described.

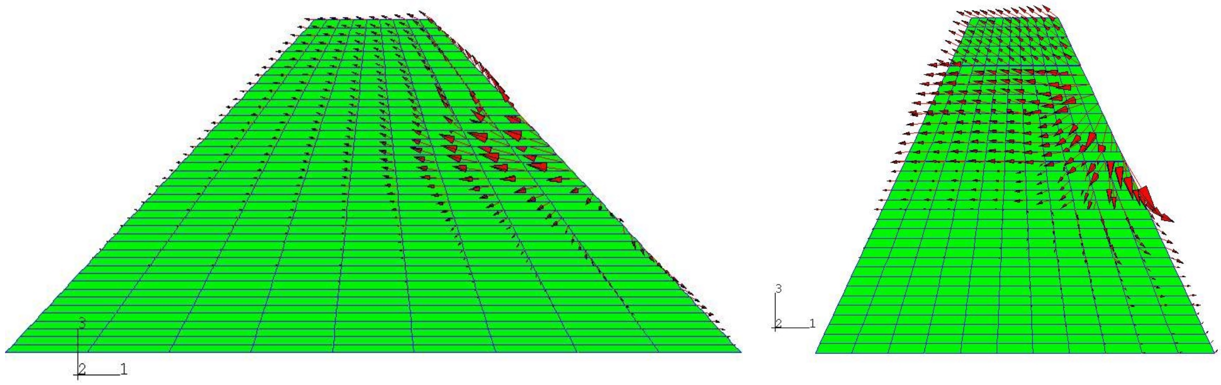

Fig. 9: comparison beetween displacements in reinforced (right) and non reinforced (left) walls

The boulder has been arrested, but large deformations (75 cm for the front penetration and 54 cm of back extrusion) have show off, with a differential pattern similar to the other reinforced wall. The contact time is more than 160 ms, proving a more ductile behavior than the first case, which results in a smaller stopping force applied to the boulder.

This is also shown by the acceleration diagrams (fig.10), in which lower peak acceleration and longer decay can be underlined in case of weak geotechnical parameters, thus meaning a more ductile global dynamic behavior.

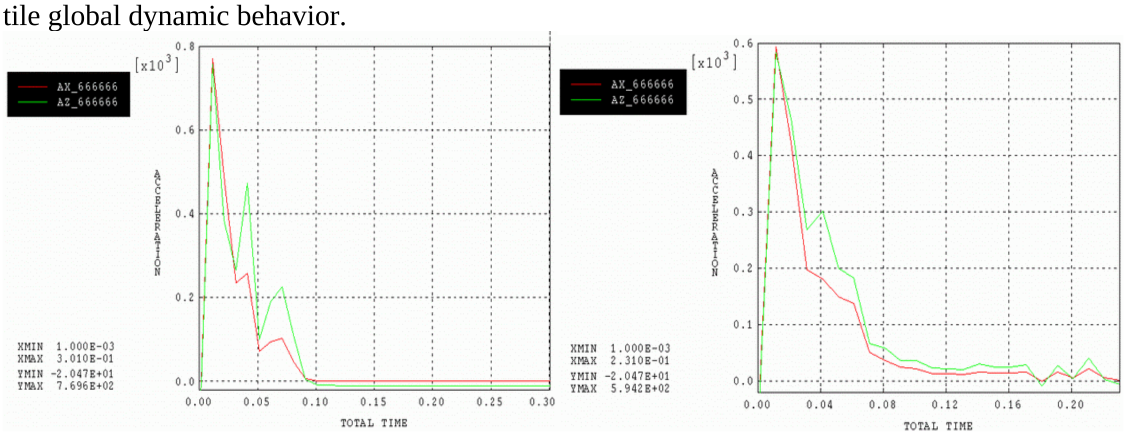

Fig. 10: comparison between block's deceleration with actual (left) and weak (right) geotechnical parameters.

3 CLOSED FORM MODEL

The mathematical model of the behavior of a reinforced soil structure subject to the impact load of a large rigid boulder can be divided in 3 parts:

- inelastic impact and sudden loss of energy;
- rigid displacement;
- energy dissipation due to deformation of the reinforced soil structure (and boulder fracture).

3.1 *Inelastic impact and loss of energy*

As known, a collision is said completely inelastic if, after collision, the two bodies stick together to form a single new body. We can easily suppose that in case of impact of a large boulder at very high speed (that is the case of practical interest), the boulder is encapsulated in the soil mass until the impact has exhausted all its effects.

Therefore, considering the impact as perfectly inelastic is equivalent to say that the coefficient of restitution *k* is equal to zero. The kinetic energy of the boulder before the impact is:

$$T_0 = \frac{1}{2} m_v \, v_v^2 \qquad (1)$$

where: m_v, v_v = Block's mass and impact velocity.

The common velocity of the boulder-soil mass, after the impact and the encapsulation of the boulder into the soil, can be found by imposing the conservation of the momentum of the translational motion, remembering that the restitution coefficient is nil:

$$v = \frac{m_r \ v_r}{m_r + m_w} \tag{2}$$

where: v = common velocity of the boulder-soil mass;
m_w = mass of the soil

The definition of m_w, that is the mass of the reinforced soil structure which is affected by the impact, can be solved only by observation of full scale tests and the related FEM modeling.

The residual kinetic energy of the boulder-soil system, after the impact, can be easily calculated by expressing the kinetic energy T_1 of such system just after the collision:

$$\begin{aligned} T_1 &= \frac{1}{2}\left(m_w + m_v\right) \cdot v^2 = \\ &= \frac{1}{2}\frac{m_r^2 \ v_r^2}{m_r + m_w} = \frac{m_r}{m_r + m_w} \cdot \frac{m_r v_r^2}{2} \end{aligned} \tag{3}$$

The residual energy is therefore given by:

$$T_1 / T_0 = \frac{m_r}{m_v + m_w} \tag{4}$$

In any case it will be: $m_w >> m_r$. Hence:

- the small part T_1 of the initial energy is spent for the rigid rotational motion of the boulder-soil system, which can be seen both in the vertical barrier reported in Burroughs et Al. (1993) shown in Fig. 2, and in the reinforced embankment shown in Fig. 5;
- the main part of the energy (T_0-T_1) is spent for the deformation of the colliding bodies. As an example, for the vertical barrier of Fig. 2 T_1 is only 2.5% of T_0.

3.2 *Residual rigid displacement*

Let's make a distinction between:

(i) structures with vertical front and back faces, stiffened by horizontal wood or metal faces, like the one in Fig. 2;
(ii) structures with inclined and almost perfectly flexible faces, like the one in Fig. 3.

Let's also suppose that the impact produces a rigid rotation of the reinforced soil structure, as it can be seen in Fig. 2.

In the first case (i) the center of rotation is moved downward in respect to the impact area, due to the stiffness of the face.

In the second case (ii) the center of rotation can be placed immediately under the impact area, hence the lower part of the structure is not affected by any rotation.

Considering now the case (i) easier to be modeled (but the same procedure can be extended to case (ii)), the "angular momentum" of the boulder-soil system before (suffix "b") the impact is:

$$\Gamma_{0_b} = \left(m_r \ v_r\right) \cdot h \tag{4}$$

while after (suffix "*a*") the impact it becomes:

$$\Gamma_{0_a} = (m_r \cdot v) \cdot h + \frac{m_w \ H^2}{3} \omega \tag{5}$$

where: h = distance between the center of gravity of the boulder and the center of rotation;
H = height of soil above the center of rotation;
ω = angular velocity of the boulder-wall system

(the "angular momentum" is very useful also for computational purposes. In particular, the possibility to use the angular velocity is useful in the future).

Since there is no other external action (except gravity, whose static moment about 0 is not significantly large during the impulse) during the impulse, it must be:

$$\Gamma_{0_b} = \Gamma_{0_a} \tag{6}$$

or

$$h\, m_r \cdot v + m_w \frac{H^2}{3} \omega = m_r v_r \cdot h \tag{7}$$

Given that the collision is totally anelastic, the boulder is captured by the soil structure, resulting in a velocity

$$v = \omega \cdot h \tag{8}$$

Then Eq. (7) becomes:

$$\omega = \frac{m_r \cdot h \cdot v_r}{\left(h^2 m_r + m_\omega \cdot \frac{H_2}{3} \right)} \tag{9}$$

Since:

$$T_1 = \frac{1}{2} I_0 \cdot \omega^2 \tag{10}$$

with: $$I_0 = m_r h^2 + m_\omega \cdot \frac{H_2}{3} \tag{11}$$

Then Eqs. (9)-(11) allow to calculate ω. The motion of the system is arrested when the residual energy T_1 equals the work dissipated by the coulombian friction between the soil and the reinforcement layers.

The shear stress of the soil-reinforcement interface is:

$$\tau = \sigma_v \ \tan \varphi \cdot f_{ds} \tag{12}$$

where: σ_v = vertical stress in the soil at the considered elevation;
φ = peak friction angle of the soil;
f_{ds} = direct shear coefficient

The shear force at the i-th soil-reinforcement interface is therefore:

$$F_i = \tau_i \cdot A_i \tag{13}$$

where: A_i = area of reinforcement affected by the motion due to the impact.

Again *A* can be evaluated only by observation of full scale tests and related FEM modeling. The total work dissipated in a rotation $d\vartheta$ of the system is:

$$L = M_0 \cdot d\vartheta = \sum_1^n {}_i \ F_i \ b_i \ d\vartheta \tag{14}$$

with: M_0 = initial moment;
b_i = arm of the i-th reinforcement layer from the center of rotation

By imposing the balance equation:

$$L = T_1 \tag{15}$$

the rigid rotation $d\vartheta$ can be calculated, and therefore also the related rigid displacement

$$x_{rigid} = z\, d\vartheta \tag{16}$$

at any elevation z above the center of rotation.

The duration dt_{rigid} of the rigid rotation can be easily calculated as well:

$$dt_{rigid} = \frac{d\vartheta}{\omega} \tag{17}$$

For the structure of Fig. 2, the rigid displacement at the center of the impact area (that is at elevation z = h over the center of rotation), results equal to 180 mm, while the duration is : dt_{rigid} = 0.54.

3.3 *Deformation of the reinforced soil structure*

As a first hypothesis, we can suppose that the soil mass and the reinforcement layers involved in the motion activated by the impact, and therefore "collaborating", have the extensions shown in Fig. 11.

Again the real values shall be validated by full scale tests and FEM analyses.

For a dynamic analysis of the motion of this collaborating system, we can characterize the soil with (Carotti & Rimoldi, 1997):

- a horizontal stiffness coefficient K;
- a viscous damping coefficient C;
- a Coulomb friction force F_c We can also characterize the reinforcing layers with (Carotti & Rimoldi, 1997):
- a horizontal stiffness coefficient K_{gg};
- a viscous damping coefficient C_{gg}.

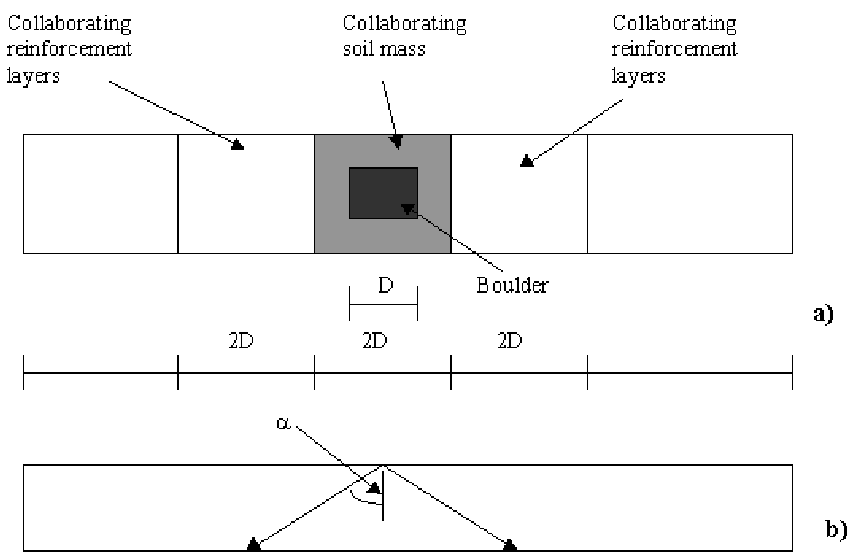

Fig. 11:First hypothesis of collaborating soil mass and reinforcement layers: a) front view; b) plan view.

These parameters in reality act in the cone limited by the angle α in Fig. 11b. With a further approximation, we can suppose that they act along the external surface of this cone. Then their component along the impact direction, supposed normal to the face, is

$$K_n = K \cdot \cos^2 \alpha \tag{18}$$

and similarly for the other coefficients.

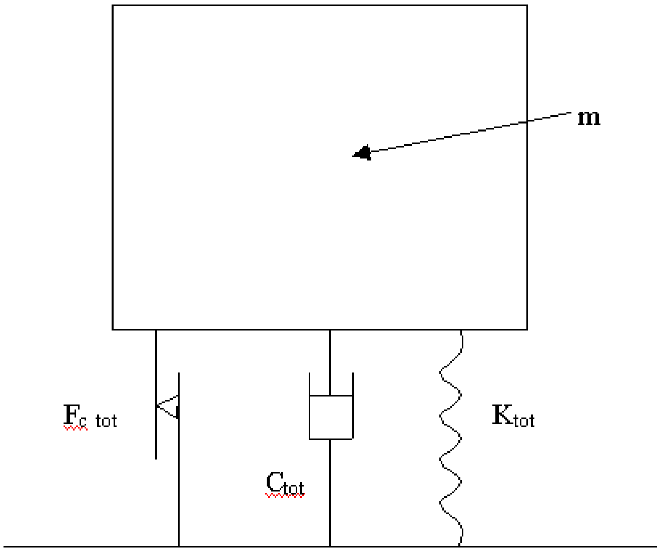

Fig. 12: Equivalent 1-DOF oscillator

Then the collaborating soil-reinforcement system can be reduced to an equivalent 1-DOF oscillator, as shown in Fig. 12, where:

$$K_{tot} = K_n + K_{gg_n} \tag{19}$$

$$C_M = C_n + C_{gg_n} \tag{20}$$

$$F_{e_{tot}} = F_{e_n} \tag{21}$$

The circular frequency of this oscillator is given by:

$$\omega = \sqrt{K_{tot}/m} \tag{22}$$

The viscous work (L_v) during a deformative cycle with maximum displacement x_d is equal to ¼ of the surface of the elliptical cycle in an ideal oscillation:

$$L_v = \frac{1}{4}\left(\pi \; C_{tot} \; \omega x_d \; x_d\right) \tag{23}$$

Since it must be:

$$L_v = T_0 - T_1 \tag{24}$$

then it is possible to obtain x_d.

The total displacement of the reinforced soil structure at any elevation is finally:

$$x_{tot}(z) = x_{rigid}(z) + x_d(z) \tag{25}$$

3.4 *Further developments*

The model illustrated above is simple and robust, but it still needs a lot of work to be defined. Further mathematical developments can be:

- models of wave propagation in the reinforced soil mass, simulated as a 3-D continuum, using standard physical-mathematical methods;
- models of wave propagation using "re-normalization groups" techniques.

4 CONCLUSIONS

Numerical and analytical methods show great potential in the analysis of a complex dynamic problem like the high energy impact of a big boulder with a reinforced soil barrier. FEM analysis of full scale tests are fundamental for defining the assumptions and validating the hypothesis required to build a closed form mathematical model. The work is just started, but the methods illustrated in the present paper seems very promising and, hopefully, they will allow in the near future to yield proper design methods for reinforced soil rock fall protection structures.

REFERENCES

Burroughs D.K., Henson H.H. e Jiang S.S. , (1993), *Full scale geotextile rock barrier wall testing, analysis and prediction,* Geosynthetics 1993, Vancouver: 959 970.

Carotti A. e Rimoldi P. ,(1998), *Parametric study for geosynthetic reinforced walls under sustained earthquakes*, Sixth International Conference on Geosynthetics, Atlanta, Georgia (USA): 25-29.

Castiglia C. (2000*), Studio del comportamento di rilevati paramassi*, Tesi di laurea (relatori: Pelizza S., Peila D., Rimoldi P.), Politecnico di Torino (non pubblicata)

Hibbit, Karlsson e Sorensen, (1998), *ABAQUS/Explicit User Manual*, Volume I.

Paronuzzi P., (1989), *Criteri di progettazione di rilevati paramassi*, Geologia tecnica, 1: 23-41

Peila D., Guasti G., Recalcati P. e Rimoldi P. (1999), *Sperimentazione su rilevati rinforzati con geogriglie per la difesa contro la caduta massi*, XX convegno Nazionale di Geotecnica, Parma

Rimoldi P, Guasti G. e Recalcati P., (1999); *I rilevati paramassi in terra rinforzata con geogriglie: applicazioni e sperimentazioni,* Convegno su "Previsione e Prevenzione di movimenti franosi rapidi", GEAM, Trento: 103-114

Rimoldi P., (1998), *Il comportamento sismico delle opere in terra rinforzata*, Atti del 12° convegno sul tema "Geosintetici nelle costruzioni in terra", AGI-IGS, pp. 37-41.

Tissières P.(1999), *Ditches and reinforced ditches against falling rocks*, Proc. Joint Japan-Swiss Scientific Seminar on Impact Loads by Rock Falls and Design of Protection Structures, Kanazawa, Japan

Yoshida H. (1999), *Recent experimental studies on rockfall control in Japan*, Proc. Joint Japan-Swiss Scientific Seminar on Impact Loads by Rock Falls and Design of Protection Structures, Kanazawa, Japan